

Original Paper

Regulation of Plasma Membrane Localization of the Na⁺-Taurocholate Co-Transporting Polypeptide by Glycochenodeoxycholate and Tauroursodeoxycholate

Patrick G. K. Mayer Natalia Qvarthava Annika Sommerfeld Boris Görg
Dieter Häussinger

Clinic for Gastroenterology, Hepatology, and Infectious Diseases, Heinrich-Heine-University,
Düsseldorf, Germany

Key Words

TUDC • GCDC • Ntcp • Integrins • Reactive oxygen species

Abstract

Background/Aims: Hydrophobic bile salts, such as glycochenodeoxycholate (GCDC) can trigger hepatocyte apoptosis, which is prevented by tauroursodesoxycholate (TUDC), but the effects of GCDC and TUDC on sinusoidal bile salt uptake via the Na⁺-taurocholate transporting polypeptide (Ntcp) are unclear. **Methods:** The effects of GCDC and TUDC on the plasma membrane localization of Ntcp were studied in perfused rat liver by means of immunofluorescence analysis and super-resolution microscopy. The underlying signaling events were investigated by Western blotting and inhibitor studies. **Results:** GCDC (20 μmol/l) induced within 60 min a retrieval of Ntcp from the basolateral membrane into the cytosol, which was accompanied by an activating phosphorylation of the Src kinases Fyn and Yes. Both, Fyn activation and the GCDC-induced Ntcp retrieval from the plasma membrane were sensitive to the NADPH oxidase inhibitor apocynin, the antioxidant N-acetylcysteine and the Src family kinase inhibitors SU6656 and PP-2, whereas PP-2 did not inhibit GCDC-induced Yes activation. Internalization of Ntcp by GCDC was also prevented by the protein kinase C (PKC) inhibitor Gö6850. TUDC (20 μmol/l) reversed the GCDC-induced retrieval of Ntcp from the plasma membrane and prevented the activation of Fyn and Yes in GCDC-perfused rat livers. Reinsertion of Ntcp into the basolateral membrane in GCDC-perfused livers by TUDC was sensitive to the protein kinase A (PKA) inhibitor H89 and the integrin-inhibitory peptide GRGDSP, whereas the control peptide GRADSP was ineffective. Exposure of cultured rat hepatocytes to GCDC (50 μmol/l, 15min) increased the fluorescence intensity of the reactive oxygen fluorescent indicator DCF to about 1.6-fold of untreated controls in a TUDC (50

µmol/l)-sensitive way. GCDC caused a TUDC-sensitive canalicular dilatation without evidence for Bsep retrieval from the canalicular membrane. **Conclusion:** The present study suggests that GCDC triggers the retrieval of Ntcp from the basolateral membrane into the cytosol through an oxidative stress-dependent activation of Fyn. TUDC prevents the GCDC-induced Fyn activation and Ntcp retrieval through integrin-dependent activation of PKA.

© 2019 The Author(s). Published by
Cell Physiol Biochem Press GmbH&Co. KG

Introduction

Liver cells express various bile salt transport proteins in order to maintain bile salt homeostasis. When the transcellular bile salt transport becomes impaired, bile salts accumulate in the hepatocyte which can trigger hepatocyte apoptosis and liver dysfunction [1-4]. The sodium taurocholate cotransporting polypeptide (Ntcp) is the major uptake system for conjugated bile salts from blood into liver parenchymal cells [5]. Secretion of bile salts at the canalicular membrane is mediated by the bile salt export pump (Bsep) [6] and by the multidrug resistance associated protein 2 (Mrp2) [7].

The expression of Bsep and Mrp2 in the apical membrane has been shown to be regulated by oxidative stress [8-10] and osmolarity [9, 11-16]. The ambient osmolarity can also regulate the cellular distribution of Ntcp in the hepatocyte. In this regard, hepatocyte swelling triggers Ntcp insertion into the membrane via activation of the phosphatidylinositol-3 kinase (PI3K)-signaling pathway and increases taurocholate (TC) uptake in hepatocytes [17], whereas hyperosmolarity induces the retrieval of Ntcp from the plasma membrane [15, 16]. This latter effect is mediated by the Src family kinase Fyn [15, 16], which is activated by a protein kinase C (PKC) ζ-dependent and nicotinamide adenine dinucleotide phosphate (NADPH) oxidase-driven formation of reactive oxygen species (ROS) [15, 16].

Cholestatic liver diseases lead to a retention of hydrophobic bile salts, such as glycochenodeoxycholate (GCDC) in the liver, which plays an important role in the pathogenesis of cholestatic liver injury [18-22].

Cholestatic disorders also trigger gene expression changes of bile salt transporters [23, 24]. While organic anion transporting protein 2 (OATP2) and Ntcp expression decreases with disease progression, MRP3 and P-glycoprotein become up-regulated. Expression of the basolateral Ntcp and Oatp2, as well as canalicular BSEP and MRP2 are also reduced in patients with acute inflammation-induced cholestasis. Retrieval of Bsep from the canalicular membrane in response to hyperosmotic hepatocyte shrinkage is accompanied by Ntcp retrieval, which is thought to counteract hepatocyte overload with bile salts when canalicular excretion fails [11, 15, 16].

Ursodeoxycholic acid (UDCA), which *in vivo* is rapidly conjugated with taurine (TUDC) has hepatoprotective and choleric effects in liver and is widely used for the treatment of cholestatic disorders, such as primary biliary cholangitis and intrahepatic cholestasis of pregnancy [25-28]. TUDC stimulates insertion of canalicular transporters into the canalicular membrane via dual activation of the MAP kinases p38^{MAPK} and Erk-1/-2 [29, 30] and exerts antiapoptotic activity [21, 31]. TUDC also counteracts internalization of Bsep [32] and Mrp2 [33] in taurocholate (TLC)-induced cholestasis. PKAα has been proposed to mediate the anti-cholestatic and antiapoptotic effects of TUDC [34]. In line with this, cyclic adenosine monophosphate (cAMP) increases Ntcp in the basolateral membrane as well as Bsep and Mrp2 in the canalicular membrane. β₁-integrins were identified as receptors for TUDC [16] and β1-integrin activation not only triggers choleresis via dual MAP kinase activation, but also is antiapoptotic through formation of cAMP and activation of protein kinase A (PKA) [31]. This prevents hyperosmotic ROS formation and Fyn activation and is associated with decreased serine phosphorylation of the Ntcp [15].

The effects of the hydrophobic bile salt GCDC on the subcellular localization of Ntcp in hepatocytes are unknown and were investigated in the present study. The results show, that GCDC triggers an oxidative stress-, and Fyn-dependent internalization of Ntcp, which is counteracted by TUDC in a β1-integrin- and PKA-dependent way.

Materials and Methods

Materials

Materials used in the present study were purchased as follows: apocynin, SU6656, PP-2, H-Gly-Arg-Gly-Asp-Ser-Pro-OH (GRGDSP) and H-Gly-Arg-Ala-Asp-Ser-Pro-OH (GRADSP) were from Merck-Millipore (Darmstadt, Germany); N-acetylcystein (NAC), Dibutyryl-cAMP (DB-cAMP) sodium salt, collagenase, insulin and TUDC were from Sigma Aldrich (Munich, Germany). H89 dihydrochloride, penicillin/streptomycin and Fluoromount-G were from Tocris/Biozol (Eching, Germany). Fetal bovine serum (FBS), G418 geneticin and Dulbecco's modified Eagle's medium Nutrimix F12 were from Life Technologies GmbH (Darmstadt, Germany). Gö6850, complete-protease inhibitor cocktail tablets and PhosSTOP-phosphatase inhibitor cocktail tablets were from Roche Diagnostics (Mannheim, Germany) and William's Medium E was from Biochrom (Berlin, Germany). The Ntcp antibody (K4) [5] was a generous gift from Prof. Dr. B. Stieger (Kantonsspital Zürich, Switzerland). The Bsep antibody was a generous gift from Professor Dr. P. J. Meier and Professor Dr. B. Stieger (University Hospital Zurich, Switzerland) [6]. The monoclonal antibody directed against ZO-1 was from Invitrogen (Karlsruhe, Germany). Antibodies recognizing Yes (immunoprecipitation, IP) and Fyn (IP) were from Santa Cruz Biotechnology (Heidelberg, Germany) and antibodies directed against c-Src were from Life Technologies GmbH (Darmstadt, Germany). The anti-phospho-serine antibody was from Enzo Life Sciences GmbH (Lörrach, Germany). The antibodies raised against phospho-Src family-Tyr-418 were from Cell Signaling Technology, Inc. (Danvers, USA), against Na⁺/K⁺-ATPase, Yes (Western blot, WB), Fyn (WB), phospho-cSrc, Cy3-conjugated donkey anti-rabbit IgG and FITC-conjugated donkey anti-mouse IgG from Merck-Millipore (Darmstadt, Germany). Horseradish peroxidase-conjugated anti-mouse IgG and anti-rabbit IgG were from Bio-Rad Laboratories (Munich, Germany) and Dako (Hamburg, Germany), respectively. All other chemicals were from Merck-Millipore (Darmstadt, Germany) at the highest quality available.

Liver perfusion

Livers from male Wistar rats (140-160 g, fed *ad libitum* with standard diet) were perfused in a non-recirculating manner with the bicarbonate-buffered Krebs-Henseleit saline plus L-lactate (2.1 mmol/l) and pyruvate (0.3 mmol/l) and equilibrated with 5% CO₂ and 95% O₂ at 37°C, as described previously [35]. Addition of bile salts, inhibitors and DB-cAMP to the influent perfusate was made by dissolution into the Krebs-Henseleit buffer.

Preparation and culture of primary rat hepatocytes

Hepatocytes were prepared from livers of male Wistar rats (160-180 g) by a collagenase perfusion technique in an adapted version as described previously [36]. Aliquots of rat hepatocytes were plated on collagen-coated culture plates and maintained in bicarbonate-buffered Krebs-Henseleit medium (115 mmol/l NaCl, 25 mmol/l NaHCO₃, 5.9 mmol/l KCl, 1.18 mmol/l MgCl₂, 1.23 mmol/l NaH₂PO₄, 1.2 mmol/l Na₂SO₄, 1.25 mmol/l CaCl₂), supplemented with 6 mmol/l glucose in a humidified atmosphere of 5% CO₂ and 95% air at 37°C. After 2 h, the medium was removed and the cells were washed twice. Subsequently the culture was continued for 24 h in William's Medium E, supplemented with 2 mmol/l glutamine, 100 nmol/l insulin, 100 U/ml penicillin, 0.1 mg/ml streptomycin, 100nmol/l dexamethasone and 5% FBS. After 24 h, experimental treatments were performed using William's Medium E that contained 2 mmol/l glutamine and 100 nmol/l dexamethasone. The viability of hepatocytes was more than 95% as assessed by trypan blue exclusion.

Immunofluorescence staining

Immunofluorescence analysis was performed as described recently [15, 16]. Tissue samples from perfused liver were cut at -20 °C in 7 µm sections using a Leica Cryotom CM 3050 (Leica, Bensheim, Germany) and placed on Superfrost plus slides (Menzel, Braunschweig, Germany). Slides were air-dried (1 h) and kept at -20 °C until staining. After fixation with pure methanol (-20 °C, 2 min), sections were washed with PBS and blocked with a solution containing 5% fetal calf serum in PBS for 30min at room temperature. Then, liver sections were incubated for 2 h in a wet chamber with combinations of primary antibodies against Ntcp (1:200) and Na⁺/K⁺-ATPase (1:200) (overnight, 4°C), washed thrice, and stained with an anti-mouse-FITC and an anti-rabbit Cy3-conjugated antibody (1:500 fetal calf serum 5% in PBS, 2 h, RT, respectively).

The samples were covered with Fluoromount-G and visualized by confocal laser scanning microscopy (LSM) using LSM510 META, the LSM880 or by super resolution structured illumination microscopy (SR-SIM) using the ELYRA microscope (Zeiss, Oberkochen, Germany).

Densitometric fluorescence intensity analysis

Densitometric fluorescence intensity analysis was performed as described recently [15, 16]. Cryosections of perfused rat liver for the analysis at the basolateral membrane were stained for Ntcp, Bsep and for Na⁺/K⁺-ATPase (plasma membrane marker protein) and ZO-1 which lines the border between the canalicular and the sinusoidal membrane. For negative controls, primary antibodies were omitted in each experiment. ZO-1 and Na⁺/K⁺-ATPase profiles were selected according apparent integrity and comparability. Acceptable Na⁺/K⁺-ATPase intensity profiles have a sufficiently high peak fluorescence in the central part (corresponding to the basolateral membrane) and low intracellular fluorescence. Densitometric analysis was performed as described previously [9, 13] using Image-Pro Plus (Media Cybernetics, Rockville, USA) software. Briefly, the fluorescence intensity profile was measured over a thick line at a right angle to the membrane. The length of the line was always 8 μm. The mean fluorescence intensity of each pixel over the line perpendicular to the length was calculated by Image-Pro Plus. The pixel intensity data (pixel positions with the associated pixel intensities, red and green channel) were transferred to an Excel data sheet (Microsoft Excel for Windows, Redmond, USA). Each measurement was normalized to the sum of all intensities of the respective measurement. Values are given as means ± SEM. Data from at least 10 different areas per tissue sample and from at least 3 independent liver preparations were processed. Peak fluorescence intensity values were statistically compared using one way analysis of variance (ANOVA) followed by Dunnett's *post hoc* test. A *p*-value <0.05 was considered statistically significant.

Western blot analysis

Western blot analysis was performed as described recently [15, 16]. Liver samples were immediately lysed at 4°C by using a lysis buffer containing 20 mmol/l Tris-HCl (pH 7.4), 140 mmol/l NaCl, 10 mmol/l NaF, 10 mmol/l sodium pyrophosphate, 1% (v/v) Triton X-100, 1 mmol/l EDTA, 1 mmol/l EGTA, 1 mmol/l sodium vanadate, 20 mmol/l β-glycerophosphate, protease inhibitor and phosphatase inhibitor cocktail. The lysates were kept on ice for 10 min and then centrifuged at 8,000 rpm for 8 min at 4°C, and aliquots of the supernatant were taken for protein determination using the Bio-Rad protein assay (Bio-Rad Laboratories, Munich, Germany). Equal amounts of protein were subjected to sodium dodecyl sulfate/polyacrylamide gel electrophoresis, and transferred onto nitrocellulose membranes using a semidry transfer apparatus (GE Healthcare, Freiburg, Germany). Membranes were blocked for 60 min in 5% (w/v) bovine serum albumin containing 20 mmol/l Tris (pH 7.5), 150 mmol/l NaCl, and 0.1% Tween 20 (TBS-T) and exposed to primary antibodies overnight at 4°C. After washing with TBS-T and incubation at RT for 2 h with horseradish peroxidase-coupled anti-mouse or anti-rabbit IgG antibody, respectively (all diluted 1:10,000), the immunoblots were washed extensively and bands were visualized using the ChemiDoc™ Touch Imaging System from Bio-Rad (Munich, Germany). Semi-quantitative evaluation was carried out by densitometry using the Image Lab Touch Software from Bio-Rad. Protein phosphorylation is given as the ratio of detected phospho-protein/total protein.

Realtime PCR analysis

Realtime PCR analysis was performed as described recently [15, 16]. Total RNA was isolated using the RNAeasy mini kit (Qiagen, Hilden, Germany) according to the manufacturers' protocol. RNA was quantified using NanoDrop1000 System (Thermo Scientific, Wilmington, USA) and first strand cDNA was synthesized from RNA using the RevertAid H Minus First Strand cDNA Synthesis Kit (Fermentas, St. Leon-Rot, Germany). Gene expression levels were quantified using SensiMix SYBR No-ROX Kit (Bioline, Luckenwalde, Germany) on a TOptical Real-Time qPCR thermal cycler (Biometra, Göttingen, Germany). Hypoxanthine-guanine phosphoribosyltransferase 1 (HPRT1) was used as reference gene for the normalization of the results obtained by the 2(-ΔΔCt) method. PCR-primer sequences: Ntcp 5'-TCAAGTCCAAAAGGCCACACT-3' and 5'-AGGGAGGAGGTAGCCAGTAAG-3', HPRT1 5'-TGCTCGAGATGTCATGAAGGA-3' and 5'-CAGAGGGCACAATGTGATG-3'. Statistical analysis was performed using one way analysis of variance (ANOVA).

Detection of Reactive Oxygen Species (ROS) in cultures hepatocytes

For detecting reactive oxygen species (ROS), hepatocytes were loaded with 2', 7'-dichlorodihydrofluorescein diacetate (H₂DCF-DA). Upon oxidation by ROS, the non-fluorescent H₂DCF is converted into the highly fluorescent 2', 7'-dichlorofluorescein (DCF). Isolated rat hepatocytes were seeded on collagen-coated 6-well culture plates and cultured for 24 h. Cells were loaded with PBS containing 5 μmol/L of H₂DCF-DA for 30 min at 37 °C and 5% CO₂. At the end of the incubation time, excess H₂DCF-DA was removed by washing the cells 3 times with culture medium (William's Medium E). Hepatocytes were pre-incubated with 50 μmol/L tauroursodeoxycholic acid (TUDC, 30 min, 5% CO₂, 37°C) before cells were exposed to glycochenodeoxycholic acid (GCDC, 50 μmol/l, 15 min, 5% CO₂, 37°C). Cells were washed 3 times with PBS and mounted on an epifluorescence microscope (Cell Observer Z1, ZEISS, Oberkochen, Germany). DCF was excited at 488 nm and fluorescence emission was collected at 565 nm. Measurements were performed in triplicate for each experimental condition and mean fluorescence intensities were corrected for background fluorescence. Emission intensity in GCDC-exposed hepatocytes is expressed relative to untreated controls. Statistical analysis was performed using one way analysis of variance (ANOVA).

Statistical analysis

Results from at least 3 independent experiments are expressed as mean values ± SEM. *n* refers to the number of independent experiments. Differences between experimental groups were analyzed by student's *t*-test, or one-way analysis of variance (ANOVA) followed by *Dunnnett's*, *Tukey's* or *Bonferroni's* multiple comparison *post hoc* test where appropriate (GraphPad Prism; GraphPad, La Jolla, USA; Microsoft Excel for Windows). A *p*-value < 0.05 was considered statistically significant.

Results

GCDC triggers Ntcp retrieval from the basolateral membrane in the perfused rat liver

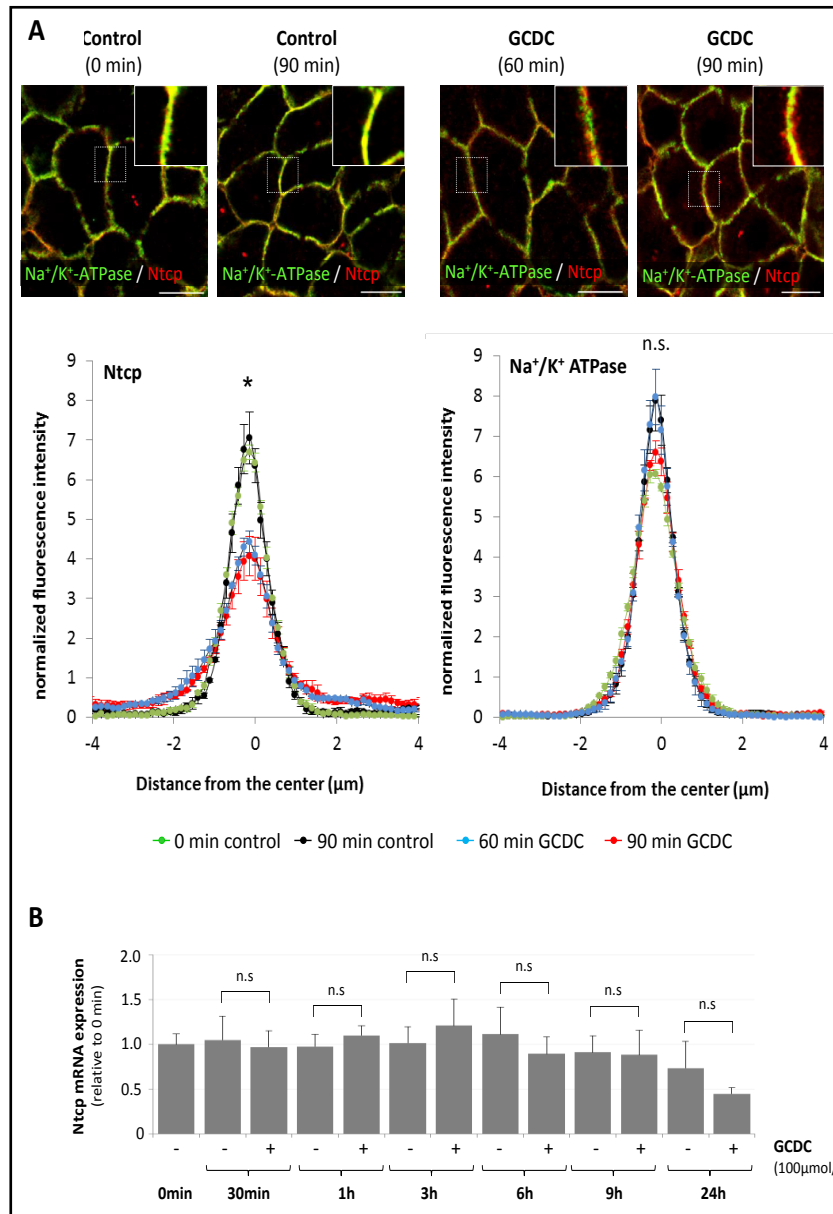
Subcellular Ntcp distribution in control and GCDC (20 μmol/l)-perfused livers was analyzed by confocal laser-scanning microscopy and quantified by densitometric analysis of fluorescence intensities as described in the methods section. For plasma membrane labelling, liver sections were stained with an antibody directed against the plasma membrane protein Na⁺/K⁺-ATPase. The immunofluorescence analysis shows that the fluorescence profiles of Ntcp shifted to significantly lower peak values and became more broadened (*p* < 0.05, Fig. 1A) in response to treatment with GCDC (20 μmol/l, 60 and 90 min), suggestive for internalization of Ntcp. In contrast, GCDC had no effect on the Na⁺/K⁺-ATPase localization (Fig. 1A). As shown in Fig. 1A by immunofluorescence microscopy, GCDC triggered the appearance of punctate Ntcp-staining, which was enriched underneath the plasma membrane, supporting the view that GCDC triggers Ntcp retrieval from the plasma membrane.

When cultured hepatocytes were exposed to GCDC, Ntcp mRNA levels remained unchanged over a 9h-period GCDC treatment (0.88 ± 0.27-fold of untreated controls, *n.s.*, *n* = 4, Fig. 1B). However, after 24h Ntcp mRNA levels tended to decrease in GCDC-exposed hepatocytes but without reaching statistical significance (0.45 ± 0.07-fold, *n* = 4, Fig. 1B).

The subcellular distribution of Ntcp was also analysed by super-resolution structured-illumination microscopy (SR-SIM) in liver slices co-stained with Ntcp and Na⁺/K⁺-ATPase (Fig. 2). In GCDC-perfused livers (20 μmol/l, 60 or 90 min), intracellular vesicular Ntcp fluorescence intensity was markedly enhanced compared to control livers. On the other hand, Na⁺/K⁺-ATPase expression at the basolateral membrane remained largely unchanged in GCDC-perfused livers (Fig. 1, 2).

These results indicate that GCDC triggers the internalisation of Ntcp in the intact rat liver within 60 min of GCDC exposure, lasting for at least 90 min.

Fig. 1. Effects of GCDC on Ntcp protein localization in rat liver and Ntcp mRNA levels in cultured hepatocytes. (A) Livers were perfused with Krebs-Henseleit buffer with or without GCDC (20 $\mu\text{mol/l}$) for up to 90 min. Cryosections of livers were immunostained for Ntcp and $\text{Na}^+/\text{K}^+\text{-ATPase}$. Fluorescence pictures were acquired by confocal laserscanning microscopy and fluorescence distribution was measured over a line (8 μm) perpendicular to the plasma membrane of adjacent hepatocytes as described in the methods section. Magnifications of the boxed regions are shown in the upper right corner of each picture. Data represent arithmetic means \pm SEM of 10 measurements in each of at least 3 individual experiments for each condition. (B) Primary rat hepatocytes were cultured for 24 h and thereafter exposed to GCDC (100 $\mu\text{mol/l}$) for up to 24 h. RNA was extracted and Ntcp mRNA expression levels were analyzed by realtime-PCR. Ntcp mRNA expression levels are given relative to the untreated control (0 min). Data represent arithmetic means \pm SEM of 4 independent experiments. * statistically significantly different compared to control. n.s.: not statistically significantly different.



thereafter exposed to GCDC (100 $\mu\text{mol/l}$) for up to 24 h. RNA was extracted and Ntcp mRNA expression levels were analyzed by realtime-PCR. Ntcp mRNA expression levels are given relative to the untreated control (0 min). Data represent arithmetic means \pm SEM of 4 independent experiments. * statistically significantly different compared to control. n.s.: not statistically significantly different.

Role of reactive oxygen species for GCDC-induced activation of Yes and Fyn in perfused rat liver

Hyperosmolarity was shown to trigger NADPH oxidase-dependent formation of reactive oxygen species (ROS) [37] and to activate the Src family kinases Yes and Fyn in the perfused rat liver [11]. Also GCDC activates NADPH oxidase and triggers the formation of ROS in cultured hepatocytes [4]. We therefore analysed effects of GCDC on the activation of Src family kinases Yes, Fyn and c-Src in perfused rat liver.

As shown in Fig. 3, the Src family kinases Yes and Fyn, but not c-Src became activated within 30 min of GCDC perfusion. The GCDC-induced Fyn and Yes activation was strongly blunted by the NADPH oxidase inhibitor apocynin (20 $\mu\text{mol/l}$) and the antioxidant NAC

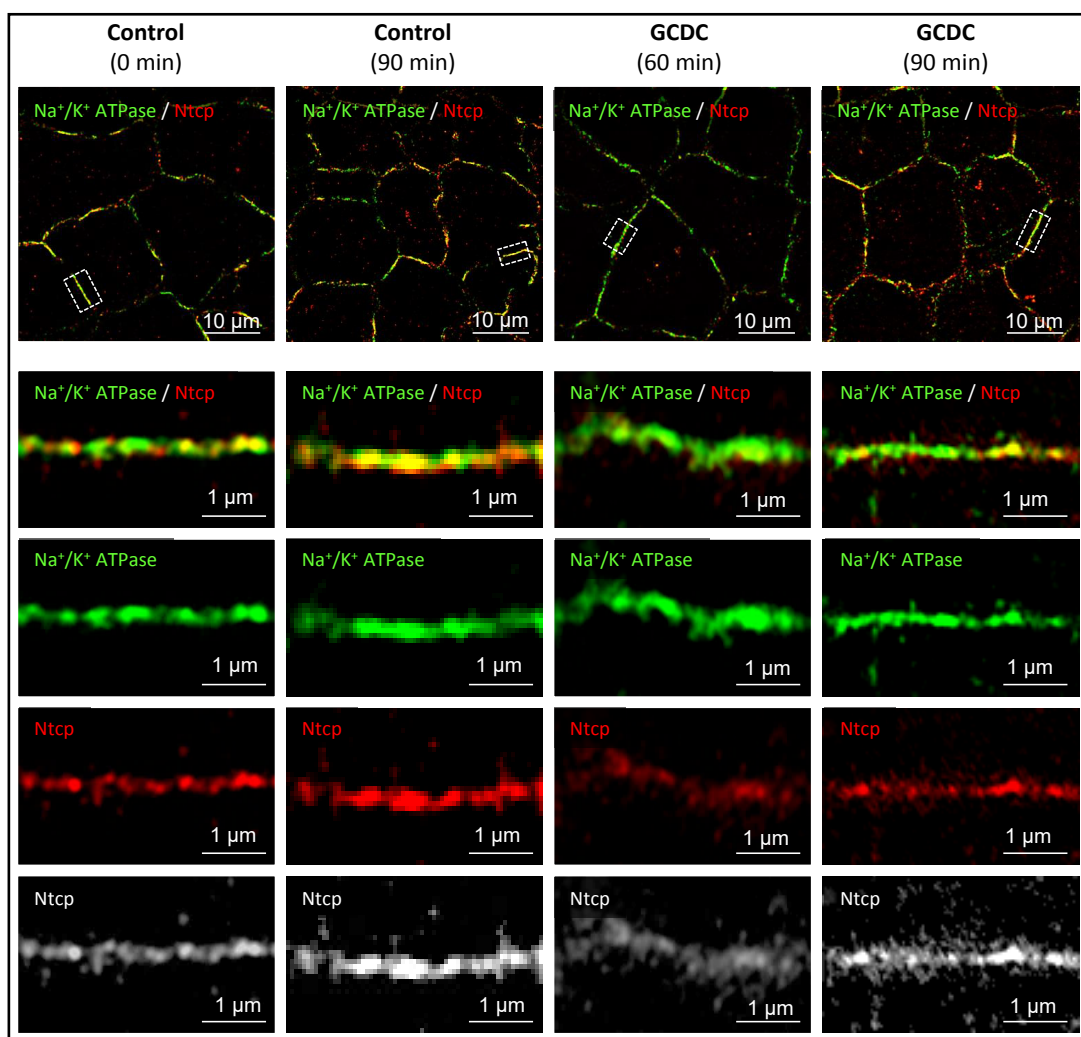


Fig. 2. Subcellular distribution of Ntcp in rat liver. Livers were perfused with Krebs-Henseleit buffer with or without GCDC (20 $\mu\text{mol/l}$) up to 90 min. Cryosections of livers were immunostained for Ntcp and Na^+/K^+ -ATPase, and analysed by SR-SIM. Representative pictures of at least 3 independent experiments are given. The scale bars correspond to 10 μm in the overviews (upper row) and 1 μm in the four bottom rows with higher magnification of the plasma membrane.

(10 mmol/l). GCDC-induced Fyn activation was largely abolished in presence of the Src kinase inhibitors SU6656 (1 $\mu\text{mol/l}$) and PP-2 (250 nmol/l), whereas GCDC-induced Yes activation was sensitive to inhibition by SU6656, but not PP-2 (Fig. 3).

The data suggest that the Src family kinases Fyn and Yes but not c-Src become activated by GCDC in a NADPH oxidase and ROS-dependent way.

Role of Fyn and Yes for the GCDC-induced retrieval of Ntcp from the basolateral membrane

The plasma membrane localization of Ntcp was analysed in GCDC (20 $\mu\text{mol/l}$)-perfused livers by laser scanning microscopy and fluorescence intensity analysis in the absence or presence of inhibitors of oxidative stress (apocynin and NAC) or Src kinases (PP-2, SU6656).

Fig. 4A depicts the liver perfusion plans chosen for these experiments. As shown in Fig. 4A and B, NAC (10 mmol/l) and apocynin (20 $\mu\text{mol/l}$) completely abolished the GCDC (20 $\mu\text{mol/l}$, 60 min)-induced Ntcp retrieval from the basolateral membrane, which was otherwise observed within 60 min (see Fig. 1A). As expected, the Na^+/K^+ -ATPase distribution remained unchanged under these conditions. Likewise, the Src kinase inhibitors SU6656

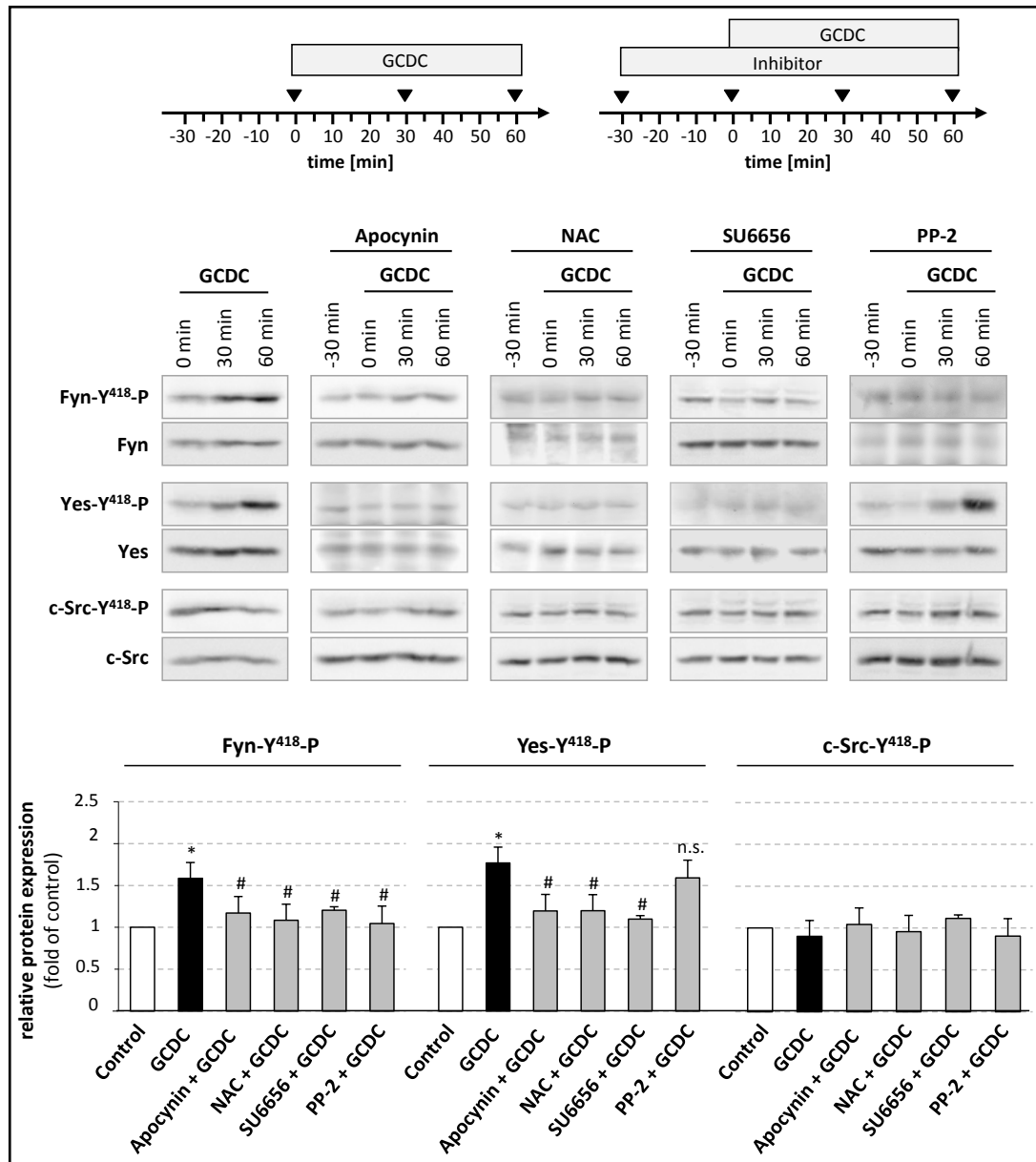


Fig. 3. Effects of GCDC on Src kinases in the perfused rat liver. Livers were perfused with Krebs-Henseleit buffer with or without GCDC (20 $\mu\text{mol/l}$) in absence or presence of apocynin (20 $\mu\text{mol/l}$), SU6656 (1 $\mu\text{mol/l}$), NAC (10 mmol/l) or PP-2 (250 nmol/l) as indicated in the perfusion plan. At the end of the experiment liver tissue was snap frozen, protein was isolated and used for Western blot analysis of activated Src kinase family members Yes, Fyn, and c-Src. Expression levels were quantified by densitometric analysis. Expression levels in livers perfused for 60 min with GCDC are given relative to what was found prior to perfusion with GCDC (0 min, "Control"). Representative blots and densitometric analysis of at least 3 independent perfusion experiments are shown. * statistically significantly different compared to control. n.s.: not statistically significantly different.

(1 $\mu\text{mol/l}$) and PP-2 (250 nmol/l) and the broad spectrum protein kinase C (PKC) inhibitor Gö6850 (10 $\mu\text{mol/l}$) prevented the GCDC-induced Ntcp retrieval from the basolateral membrane (Fig. 4B).

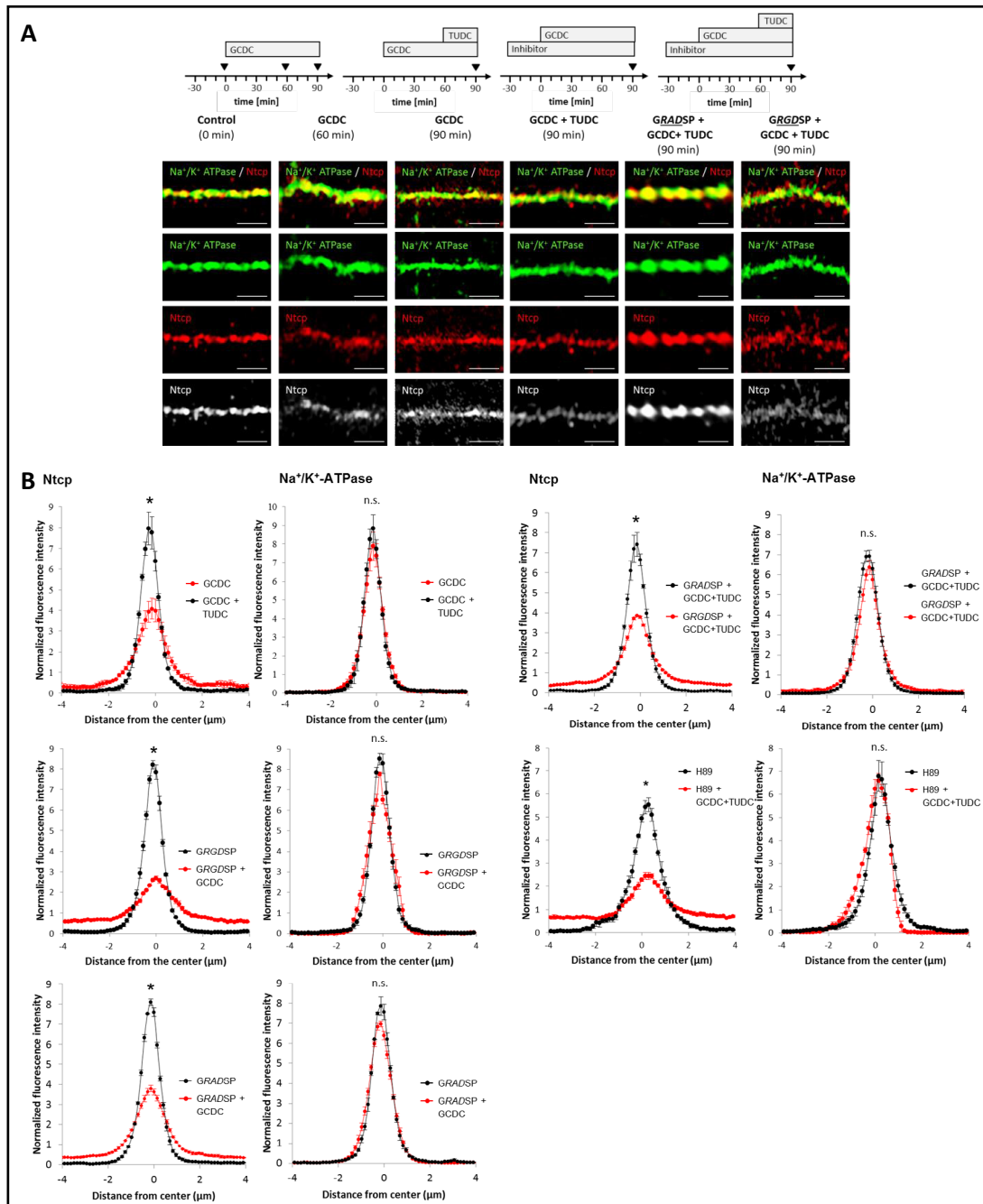


Fig. 5. TUDC reverses the GCDC-induced retrieval of Ntcp in an integrin- and PKA-dependent way. (A, B) Rat livers were perfused with GCDC (20 μmol/l), TUDC (20 μmol/l), GRGDSP (10 μmol/l), GRADSP (10 μmol/l) and/ or H89 (2 μmol/l) as indicated in the respective perfusion plans (A). Livers were fixed and Ntcp and Na⁺/K⁺-ATPase were analysed by immunofluorescence and (A) SR-SIM or (B) confocal laserscanning microscopy and Ntcp distribution was quantified as described in methods at t = 90 min. Representative images from at least 3 independent experiments are shown. The scale bars correspond to 1 μm. (B) Arithmetic means ± SEM for at least 10-30 independent measurements per animal and 3 independent experiments for each condition are shown. * statistically significantly different compared to control. n.s.: not statistically significantly different.

These findings suggest that the retrieval of Ntcp from the plasma membrane depends on activation of NADPH oxidase, ROS formation, PKC and Src kinases. Because PP-2 prevented both, GCDC-induced Ntcp retrieval and Fyn (but not Yes) activation, it is concluded that GCDC-induced Ntcp internalization is mediated by Fyn, but not by Yes. Similar observations were made regarding the hyperosmolarity-induced Ntcp retrieval [15, 16].

Tauroursodesoxycholate (TUDC) reverses GCDC-induced Ntcp internalization via activation of integrins and protein kinase A

The bile salt TUDC triggers via β_1 -integrin activation the insertion of intracellularly stored Bsep and Mrp2 into the canalicular membrane, thereby mediating a choleric effect [12, 16]. We therefore investigated the effects of TUDC on GCDC-induced retrieval of Ntcp from the basolateral membrane in perfused rat liver.

As shown by immunofluorescence analysis, the GCDC (20 $\mu\text{mol/l}$)-induced retrieval of Ntcp is reversed by TUDC (20 $\mu\text{mol/l}$) within 30 min (Fig. 5A, B). This inhibitory effect of TUDC on GCDC-induced Ntcp retrieval was fully prevented by the β_1 -integrin-inhibitory peptide GRGDSP but not by the inactive control peptide GRADSP (both 10 $\mu\text{mol/l}$) (Fig. 5B).

As shown recently, TUDC activates protein kinase A (PKA) via β_1 -integrins [31]. As shown in Fig. 5B, the PKA-inhibitor H89 (2 $\mu\text{mol/l}$) largely prevented the inhibitory effect of TUDC on GCDC-induced Ntcp retrieval. Na^+/K^+ -ATPase immunostaining remained unchanged under all conditions.

These data show that TUDC inhibits the GCDC-induced Ntcp internalization by activating integrins and PKA.

TUDC prevents GCDC-induced activation of Fyn and Yes via β_1 -integrins and PKA

Recent studies suggested, that TUDC counteracts the hyperosmolarity-induced retrieval of Ntcp through β_1 -integrin and PKA-dependent inhibition of Fyn activation [15].

As shown in Fig. 6A, the inhibitory effect of TUDC on the activation of Fyn and Yes by GCDC was fully abrogated by the inhibitory integrin antagonist GRGDSP but not by the inactive control peptide GRADSP (both 10 $\mu\text{mol/l}$). Furthermore, the inhibitory effect of TUDC on the GCDC-induced activation of Fyn and Yes was fully prevented by the PKA inhibitor H89 (2 $\mu\text{mol/l}$). The GCDC-induced activation of Fyn was also abolished in presence of dibutyryl-cAMP (50 $\mu\text{mol/l}$) (Fig. 6B). The inhibitory effect of dibutyryl-cAMP on GCDC-induced Fyn activation was fully prevented by the PKA inhibitor H89 (2 $\mu\text{mol/l}$).

The data suggest that TUDC inhibits the GCDC-induced activation of Fyn and Yes in an integrin and PKA-dependent way in the perfused rat liver.

TUDC prevents the GCDC-induced ROS formation in cultured rat hepatocytes

Effects of TUDC on GCDC-induced ROS formation were studied in $\text{H}_2\text{DCF-DA}$ -loaded rat hepatocytes by fluorescence microscopy.

As shown in Fig. 7, exposure of hepatocytes to GCDC (50 $\mu\text{mol/l}$, 15 min) strongly increased DCF fluorescence by about 2-fold compared to untreated controls. Pretreatment of the hepatocytes with TUDC (50 $\mu\text{mol/l}$, 30 min) fully prevented the GCDC-induced DCF fluorescence increase (Fig. 7). The data suggest that TUDC blocks GCDC-induced formation of reactive oxygen species in cultured rat hepatocytes.

GCDC triggers dilatation of the canaliculi in the perfused rat liver

Subcellular distribution of Bsep was analysed in perfused livers by confocal laser-scanning microscopy (Fig. 8A) and quantified by densitometric analysis of fluorescence intensities (Fig. 8B, C). For labelling of the canalicular membrane, liver sections were stained with an antibody directed against the tight junction protein zonula occludens 1 (ZO-1). Fluorescence profiles of Bsep shifted to significantly lower peak values and became more broadened in GCDC-perfused livers ($p < 0.05$, Fig. 8B) in response to treatment with GCDC (20 $\mu\text{mol/l}$, 90 min), which may at first glance suggest an internalization of Bsep. However, GCDC also significantly increased the distance between the ZO-1 immunoreactivities

Fig. 6. TUDC inhibits integrin- and PKA-dependently the GCDC-induced activation of Fyn. Rat livers were perfused with TUDC (20 $\mu\text{mol/l}$) or GCDC (20 $\mu\text{mol/l}$) either in absence or presence of (A) GRGDSP (10 $\mu\text{mol/l}$), GRADSP (10 $\mu\text{mol/l}$) or H89 (2 $\mu\text{mol/l}$) or (B) cAMP and/or H89 as indicated in the perfusion plans. Liver samples were analyzed for phosphorylation of the Src kinases Fyn and Yes by Western blot. Fyn and Yes phosphorylation was quantified by densitometric analysis at $t = 90 \text{ min}$ ($n \geq 3$). * statistically significantly different compared to control. n.s.: not statistically significantly different.

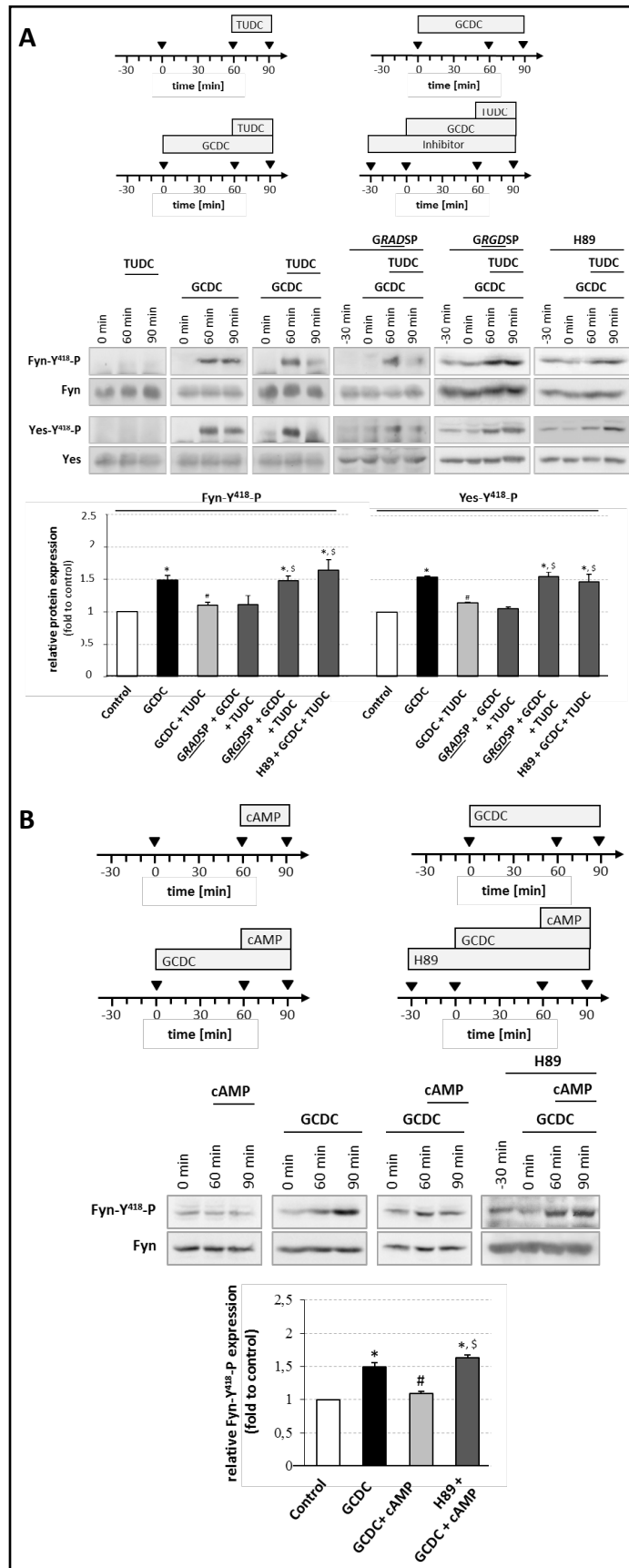
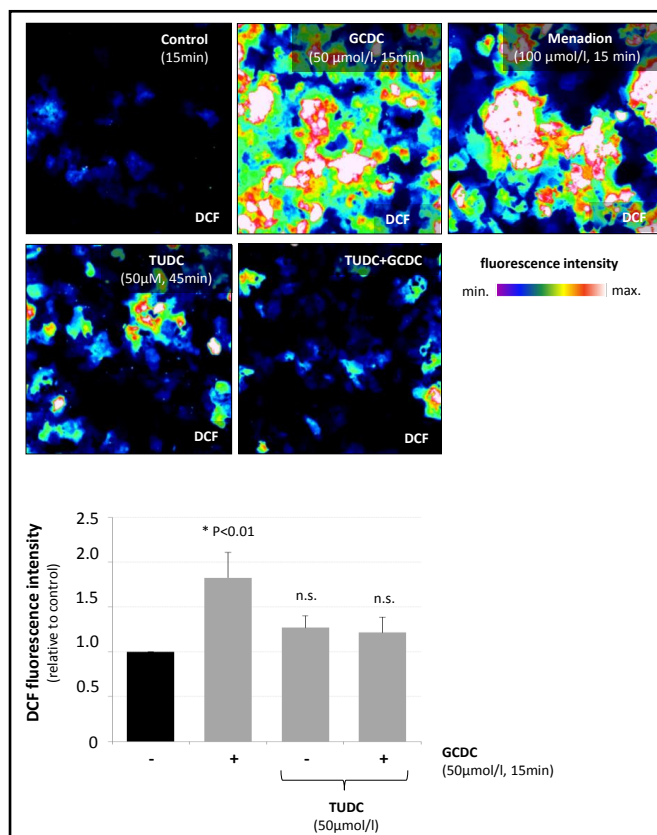


Fig. 7. TUDC blocks the GCDC-induced formation of reactive oxygen species. Primary rat hepatocytes were cultured for 24 h, loaded with DCF as described in materials and methods and exposed to GCDC (50 $\mu\text{mol/l}$) for 15 min. Where indicated, hepatocytes were pre-incubated with TUDC (50 $\mu\text{mol/l}$) for 30 min before hepatocytes were exposed to GCDC in the presence of TUDC. Fluorescence was collected by epifluorescence microscopy and fluorescence intensities were quantified using AxioVision Software. ROS levels in GCDC or TUDC-exposed hepatocytes are given relative to the control. Data are mean values \pm SEM of $n \geq 3$ independent experiments. * statistically significantly different compared to the untreated control. n.s.: not statistically significantly different.



lining the canalicular membrane (Fig. 8A, B, C). However, no punctate Bsep-staining was detected in the cytosol underneath the canalicular membrane in GCDC-perfused livers in confocal microscopy (Supplementary Fig. 1 - for all supplemental material see www.cellphysiolbiochem.com). Thus, the flattening of the Bsep fluorescence profile is due to a dilatation of the canalculus, whereas retrieval of Bsep from the canalicular membrane was not observed. Both, the GCDC-induced broadening of the Bsep profile as well as the dilatation of the canalculus were fully reversed by TUDC (20 $\mu\text{mol/l}$) (Fig. 8A-C). These inhibitory effects of TUDC were fully prevented by the integrin inhibitory peptide *GRGDSP* but not by its inactive analogon *GRADSP* (10 $\mu\text{mol/l}$) (Fig. 8A-C).

These results indicate that GCDC triggers a dilatation of the canalculus, which is counteracted by TUDC through activation of $\beta 1$ -integrins.

Discussion

Bile salt homeostasis is achieved through adaptive activity changes of bile salt transporters in the hepatocyte membrane [38]. Short-term regulation of bile salt transporters involves substrate availability [39], covalent modifications [40, 41] or rapid insertion/retrieval of transporters into/from the sinusoidal and canalicular membrane [9, 29, 42, 43], whereas long-term adaption involves transcriptional or translational changes in transporter expression [44-47]. During cholestasis bile salt transporters can undergo a hepatoprotective adaptive regulation [48, 49]. In the present study, we analysed short-term effects of GCDC on the cellular localization of the bile salt transporter Na^+ -taurocholate cotransporting polypeptide (Ntcp) in the perfused rat liver. The data show, that GCDC triggers the rapid retrieval of Ntcp from the basolateral membrane. This process involves PKC, NADPH oxidase-derived ROS and activation of the Src family kinase Fyn. Whereas GCDC-induced Ntcp internalization and Fyn activation were prevented by both, PP-2 and SU6656, Yes activation

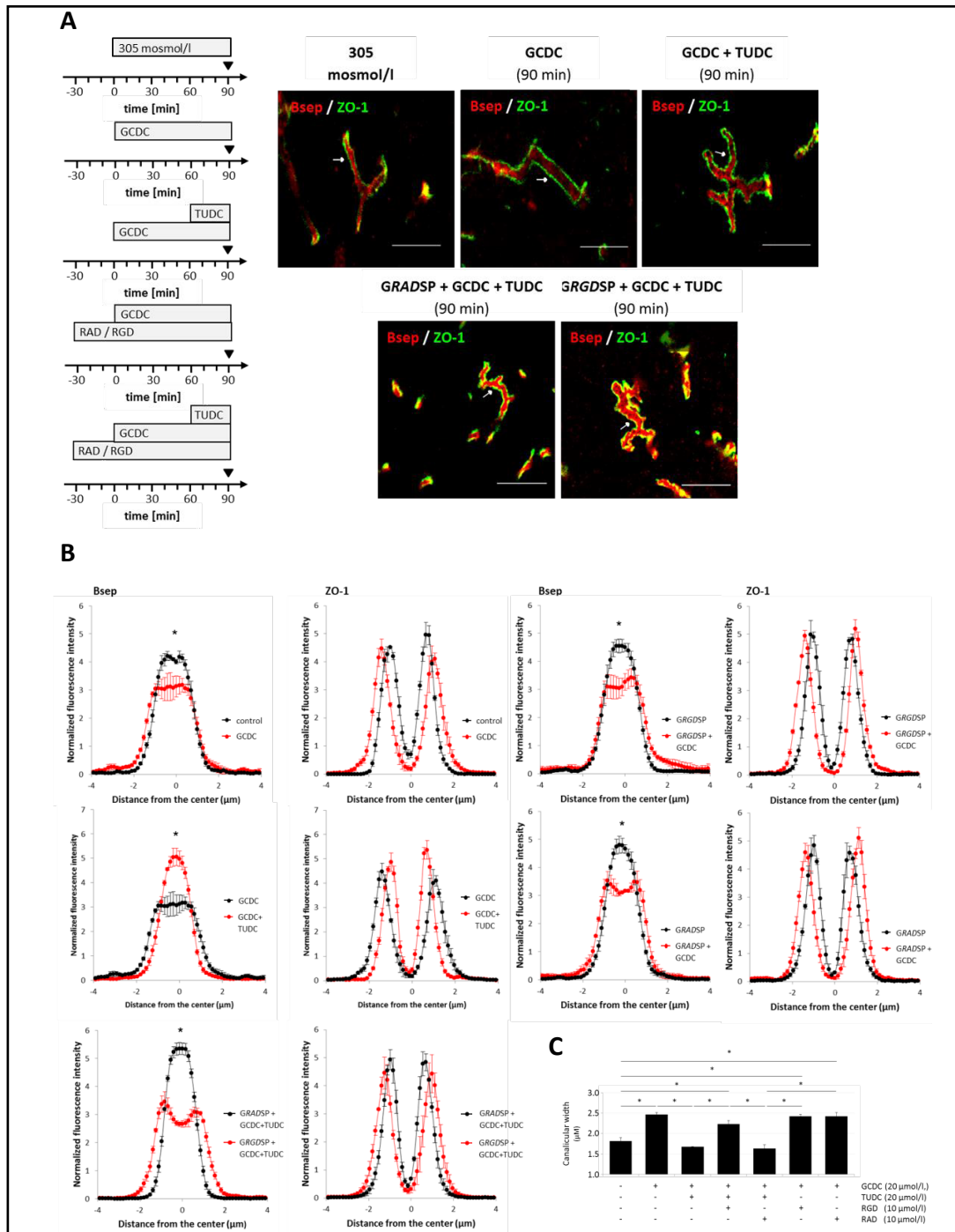


Fig. 8. Effects of GCDC on the subcellular distribution of Bsep and ZO-1 in perfused rat liver. Rat livers were perfused with Krebs-Henseleit buffer in presence or absence of GCDC (20 µmol/l) and/or TUDC (20 µmol/l), GRGDSP (10 µmol/l) and/or GRADSP (10 µmol/l) as indicated in the perfusion plan. (A) Bsep and ZO-1 were visualized by confocal laserscanning microscopy at t = 90 min. Representative images from 3 independent experiments are shown. The scale bar corresponds to 10 µm. (B) Densitometric analysis of fluorescence intensity profiles of Bsep and ZO-1 staining at t = 90 min. GCDC induces dilatation of the canaliculi as suggested by an increased distance between the ZO-1 peaks. (C) Canaliculus width as measured by the distance of ZO-1 peak immunoreactivities between the canalicular borders. Data consist of arithmetic means ± SEM of 10-30 measurements in each of 3 individual experiments for each condition. * statistically significantly different to control.

was only sensitive to SU6656. This suggests that Fyn, but not Yes is involved in retrieval of Ntcp from the basolateral membrane. Activated Fyn in turn may phosphorylate Ntcp in the GCDC-perfused liver and thereby trigger internalization of the transporter [15, 16].

Similar to the recently described role of ROS for activation of Fyn during hyperosmotic hepatocyte shrinkage [15, 16], also GCDC-induced Fyn activation is the consequence of NADPH oxidase-dependent ROS formation in cultured hepatocytes [4, 50]. In line with this, inhibition of NADPH oxidase by apocynin and the antioxidant N-acetylcysteine prevented Fyn activation and the GCDC-induced Ntcp internalization. Retrieval of Ntcp from the plasma membrane was also recently found in response to the hydrophobic bile salt taurochenodesoxycholate (TCDC), but the underlying mechanism may differ from the one identified for GCDC in the present study. The TCDC-induced internalization depends on activation of PKC and protein phosphatase 2A, is inhibited by PI3K and importantly ROS are not involved [51].

Interestingly, the GCDC-induced internalization of Ntcp was fully counteracted by the anti-cholestatic bile salt TUDC in a β_1 -integrin and PKA-dependent way. As shown in the present study, TUDC prevented the GCDC-induced ROS formation (as assessed by DCF fluorescence) and Fyn activation, as it was previously also observed for hyperosmotic ROS formation [15, 16]. This, however, is at variance to our recent finding showing that TUDC had no effect on the GCDC-induced p47^{phox} phosphorylation [31]. The reason for this is unclear, but may reflect different approaches for assessment of oxidative stress (DCFDA fluorescence vs. p47^{phox} phosphorylation) and apart from Nox further ROS generating compartments such as mitochondria may be picked up when measuring TUDC effects using DCFDA fluorescence. In line with this, it was shown that ursodesoxycholate can counteract the deoxycholic acid-induced ROS response by preventing mitochondrial membrane permeability transition [52]. Clearly, TUDC prevents GCDC-induced Fyn activation in a β_1 -integrin and PKA-dependent way, but it is unclear, whether these responses are primarily due to an antioxidative action of TUDC.

As shown recently, TUDC directly activates β_1 -integrins and thereby stimulates the formation of cAMP [31], whose choleric effect is well-known. cAMP increases transcellular bile salt transport by upregulating the Ntcp in the basolateral membrane [53] and increasing the levels of Mrp2 [54] and Bsep in the canalicular membrane [55]. The choleric effect of cAMP may be due to a PKA-mediated PI3K activation [56], which leads to the activation of Akt and PKC isoforms [56-59] and induces Ntcp targeting to the plasma membrane. Moreover, the cAMP-induced insertion of Ntcp into the plasma membrane is associated with a serine dephosphorylation of Ntcp [42, 60] and the cAMP-induced activation of protein phosphatase 2B can directly dephosphorylate Ntcp [61]. Thus, Ntcp targeting to the plasma membrane by TUDC may not only reside in a prevention of GCDC-induced Fyn phosphorylation, but also in a β_1 -integrin-dependent cAMP formation. In line with this, TUDC-induced reinsertion of Ntcp into the plasma membrane in GCDC perfused livers was sensitive to inhibition of β_1 -integrins as well as to inhibition of PKA. These data also corroborate earlier findings showing that TUDC stimulates Ntcp reinsertion into the plasma membrane under hyperosmotic conditions in a β_1 -integrin-dependent way [15, 16]. Interestingly, the mechanisms underlying the GCDC-induced internalization of Ntcp, as shown in the present study, strongly resembles the ones triggering Ntcp retrieval from plasma membrane in hyperosmotically-perfused livers [15, 16]. Therefore it seems reasonable to speculate that GCDC-induced hepatocyte shrinkage [4] may contribute to Ntcp internalization. As shown recently, hyperosmolarity triggers a coordinated Fyn-dependent Ntcp and Bsep retrieval from the respective membranes. Because GCDC also activates Fyn, not only Ntcp retrieval, but also Bsep retrieval under the influence of GCDC may be anticipated. However, in contrast to hyperosmolarity [11], GCDC induced not only a broadening of the Bsep fluorescence profile, but also a significant dilatation of the canalculi, which by itself may already explain the flattening of the Bsep fluorescence profile. In line with this, no Bsep retrieval from the canalicular membrane was observed in response to GCDC. Canalicular dilatation has also been described in response to tauroolithocholate [62-64], to ischemia-reperfusion injury [65], chlorpromazine and estradiol-17 β -D-glucuronide

[66]. The mechanisms underlying the GCDC-induced widening of the canaliculi remain speculative and may involve oxidative stress-effects on the cytoskeleton of hepatocytes. Interestingly, GCDC-induced canalicular dilatation was prevented by TUDC and similar observations were reported in drug-induced cholestasis and after ischemia-reperfusion [65, 66].

Conclusion

Taken together, the results of the present study suggest that the cholestatic bile salt GCDC not only triggers a proapoptotic state [38], but also inhibits the uptake of bile salts by hepatocytes, which may reflect a hepatoprotective response (Supplementary Fig. 2).

Abbreviations

Bsep (bile salt export pump); cAMP (cyclic adenosine monophosphate); DB-cAMP (dibutyryl-cAMP); H₂DCFDA (dihydro-2',7'-dichlorofluorescein-diacetate); DCF (2',7'-dichlorofluorescein); GCDC (glycochenodeoxycholate); GRGDSP (RGD motif containing hexapeptide); GRADSP (inactive control peptide of RAD motif containing hexapeptide); HPRT (hypoxanthine-guanine phosphoribosyltransferase); LSM (laser scanning microscopy); MAPK (mitogen activated protein kinase); Mrp2 (multidrug resistance associated protein 2); NAC (N-acetylcysteine); NADPH (reduced form of nicotinamide adenine dinucleotide phosphate); Ntcp (Na⁺-taurocholate cotransporting polypeptide); OATP2 (organic anion transporting polypeptide 2); PBC (primary biliary cholangitis); PI3K (phosphatidylinositol 3 kinase); PKA (protein kinase A); PKC (protein kinase C); PSC (primary sclerosing cholangitis); ROS (reactive oxygen species); SR-SIM (Super-resolution structured-illumination microscopy); TC (taurocholate); TCDC (taurochenodeoxycholate); TLC (tauro lithocholate); TUDC (tauroursodeoxycholate); ZO-1 (zonula occludens 1).

Acknowledgements

The authors are grateful to Nicole Eichhorst, Lisa Knopp and Janina Thies for expert technical assistance. Funded by the Deutsche Forschungsgemeinschaft (DFG, German Research Foundation) – Projektnummer 190586431 – SFB 974 „Communication and Systems Relevance during Liver Damage and Regeneration“ (Düsseldorf). All animal experiments were approved by the responsible local authorities of the “Zentrale Einrichtung für Tierforschung und wissenschaftliche Tierschutzaufgaben” (ZETT) of the University of Düsseldorf and the “Landesamt für Natur, Umwelt und Verbraucherschutz Nordrhein-Westfalen” (LANUV, NRW).

Disclosure Statement

The authors declare that they have no conflicts of interest with the content of this article.

References

- 1 Elferink RO, Groen AK: Genetic defects in hepatobiliary transport. *Biochim Biophys Acta* 2002;1586:129-145.

- 2 Watanabe M, Houten SM, Matak C, Christoffolete MA, Kim BW, Sato H, Messaddeq N, Harney JW, Ezaki O, Kodama T, Schoonjans K, Bianco AC, Auwerx J: Bile acids induce energy expenditure by promoting intracellular thyroid hormone activation. *Nature* 2006;439:484-489.
- 3 Graf D, Kohlmann C, Haselow K, Gehrmann T, Bode JG, Häussinger D: Bile acids inhibit interleukin-6 signaling via gp130 receptor-dependent and -independent pathways in rat liver. *Hepatology* 2006;44:1206-1217.
- 4 Becker S, Reinehr R, Graf D, vom Dahl S, Häussinger D: Hydrophobic bile salts induce hepatocyte shrinkage via NADPH oxidase activation. *Cell Physiol Biochem* 2007;19:89-98.
- 5 Stieger B, Hagenbuch B, Landmann L, Hochli M, Schroeder A, Meier PJ: In situ localization of the hepatocytic Na⁺/Taurocholate cotransporting polypeptide in rat liver. *Gastroenterology* 1994;107:1781-1787.
- 6 Gerloff T, Stieger B, Hagenbuch B, Madon J, Landmann L, Roth J, Hofmann AF, Meier PJ: The sister of P-glycoprotein represents the canalicular bile salt export pump of mammalian liver. *J Biol Chem* 1998;273:10046-10050.
- 7 Akita H, Suzuki H, Ito K, Kinoshita S, Sato N, Takikawa H, Sugiyama Y: Characterization of bile acid transport mediated by multidrug resistance associated protein 2 and bile salt export pump. *Biochim Biophys Acta* 2001;1511:7-16.
- 8 Schmitt M, Kubitz R, Wettstein M, vom Dahl S, Häussinger D: Retrieval of the mrp2 gene encoded conjugate export pump from the canalicular membrane contributes to cholestasis induced by tert-butyl hydroperoxide and chloro-dinitrobenzene. *Biol Chem* 2000;381:487-495.
- 9 Schmitt M, Kubitz R, Lizun S, Wettstein M, Häussinger D: Regulation of the dynamic localization of the rat Bsep gene-encoded bile salt export pump by anisoosmolarity. *Hepatology* 2001;33:509-518.
- 10 Perez LM, Milkiewicz P, Elias E, Coleman R, Sanchez Pozzi EJ, Roma MG: Oxidative stress induces internalization of the bile salt export pump, Bsep, and bile salt secretory failure in isolated rat hepatocyte couplets: a role for protein kinase C and prevention by protein kinase A. *Toxicol Sci* 2006;91:150-158.
- 11 Cantore M, Reinehr R, Sommerfeld A, Becker M, Häussinger D: The Src family kinase Fyn mediates hyperosmolarity-induced Mrp2 and Bsep retrieval from canalicular membrane. *J Biol Chem* 2011;286:45014-45029.
- 12 Häussinger D, Kurz AK, Wettstein M, Graf D, Vom Dahl S, Schliess F: Involvement of integrins and Src in tauroursodeoxycholate-induced and swelling-induced cholestasis. *Gastroenterology* 2003;124:1476-1487.
- 13 Kubitz R, D'Urso D, Keppler D, Häussinger D: Osmodependent dynamic localization of the multidrug resistance protein 2 in the rat hepatocyte canalicular membrane. *Gastroenterology* 1997;113:1438-1442.
- 14 Warskulat U, Kubitz R, Wettstein M, Stieger B, Meier PJ, Häussinger D: Regulation of bile salt export pump mRNA levels by dexamethasone and osmolarity in cultured rat hepatocytes. *Biol Chem* 1999;380:1273-1279.
- 15 Sommerfeld A, Mayer PG, Cantore M, Häussinger D: Regulation of plasma membrane localization of the Na⁺-taurocholate cotransporting polypeptide (Ntcp) by hyperosmolarity and tauroursodeoxycholate. *J Biol Chem* 2015;290:24237-24254.
- 16 Gohlke H, Schmitz B, Sommerfeld A, Reinehr R, Häussinger D: alpha5 beta1-integrins are sensors for tauroursodeoxycholic acid in hepatocytes. *Hepatology* 2013;57:1117-1129.
- 17 Webster CR, Blanch CJ, Phillips J, Anwer MS: Cell swelling-induced translocation of rat liver Na(+)/taurocholate cotransport polypeptide is mediated via the phosphoinositide 3-kinase signaling pathway. *J Biol Chem* 2000;275:29754-29760.
- 18 Kaplan MM, Gershwin ME: Primary biliary cirrhosis. *N Engl J Med* 2005;353:1261-1273.
- 19 Zollner G, Trauner M: Mechanisms of cholestasis. *Clin Liver Dis* 2008;12:1-26, vii.
- 20 Fickert P, Moustafa T, Trauner M: Primary sclerosing cholangitis-the arteriosclerosis of the bile duct? *Lipids Health Dis* 2007;6:3.
- 21 Reinehr R, Becker S, Wettstein M, Häussinger D: Involvement of the Src family kinase yes in bile salt-induced apoptosis. *Gastroenterology* 2004;127:1540-1557.
- 22 Reinehr R, Graf D, Häussinger D: Bile salt-induced hepatocyte apoptosis involves epidermal growth factor receptor-dependent CD95 tyrosine phosphorylation. *Gastroenterology* 2003;125:839-853.
- 23 Zollner G, Fickert P, Zenz R, Fuchsbichler A, Stumptner C, Kenner L, Ferenci P, Stauber RE, Krejs GJ, Denk H, Zatloukal K, Trauner M: Hepatobiliary transporter expression in percutaneous liver biopsies of patients with cholestatic liver diseases. *Hepatology* 2001;33:633-646.
- 24 Zollner G, Fickert P, Silbert D, Fuchsbichler A, Marschall HU, Zatloukal K, Denk H, Trauner M: Adaptive changes in hepatobiliary transporter expression in primary biliary cirrhosis. *J Hepatol* 2003;38:717-727.

- 25 Beuers U, Spengler U, Kruis W, Aydemir U, Wiebecke B, Heldwein W, Weinzierl M, Pape GR, Sauerbruch T, Paumgartner G: Ursodeoxycholic acid for treatment of primary sclerosing cholangitis: a placebo-controlled trial. *Hepatology* 1992;16:707-714.
- 26 Leuschner U, Fischer H, Kurtz W, Guldutuna S, Hubner K, Hellstern A, Gatzem M, Leuschner M: Ursodeoxycholic acid in primary biliary cirrhosis: results of a controlled double-blind trial. *Gastroenterology* 1989;97:1268-1274.
- 27 Poupon R: Ursodeoxycholic acid and bile-acid mimetics as therapeutic agents for cholestatic liver diseases: an overview of their mechanisms of action. *Clin Res Hepatol Gastroenterol* 2012;36:S3-12.
- 28 Poupon RE, Balkau B, Eschwege E, Poupon R: A multicenter, controlled trial of ursodiol for the treatment of primary biliary cirrhosis. UDCA-PBC Study Group. *N Engl J Med* 1991;324:1548-1554.
- 29 Kurz AK, Graf D, Schmitt M, Vom Dahl S, Häussinger D: Tauroursodesoxycholate-induced choleresis involves p38(MAPK) activation and translocation of the bile salt export pump in rats. *Gastroenterology* 2001;121:407-419.
- 30 Schliess F, Kurz AK, vom Dahl S, Häussinger D: Mitogen-activated protein kinases mediate the stimulation of bile acid secretion by tauroursodeoxycholate in rat liver. *Gastroenterology* 1997;113:1306-1314.
- 31 Sommerfeld A, Reinehr R, Häussinger D: Tauroursodeoxycholate Protects Rat Hepatocytes from Bile Acid-Induced Apoptosis via β 1-Integrin- and Protein Kinase A-Dependent Mechanisms. *Cell Physiol Biochem* 2015;36:866-883.
- 32 Dombrowski F, Stieger B, Beuers U: Tauroursodeoxycholic acid inserts the bile salt export pump into canalicular membranes of cholestatic rat liver. *Lab Invest* 2006;86:166-174.
- 33 Beuers U, Bilzer M, Chittattu A, Kullak-Ublick GA, Keppler D, Paumgartner G, Dombrowski F: Tauroursodeoxycholic acid inserts the apical conjugate export pump, Mrp2, into canalicular membranes and stimulates organic anion secretion by protein kinase C-dependent mechanisms in cholestatic rat liver. *Hepatology* 2001;33:1206-1216.
- 34 Beuers U, Denk GU, Soroka CJ, Wimmer R, Rust C, Paumgartner G, Boyer JL: Tauroolithocholic acid exerts cholestatic effects via phosphatidylinositol 3-kinase-dependent mechanisms in perfused rat livers and rat hepatocyte couplets. *J Biol Chem* 2003;278:17810-17818.
- 35 Sies H: The use of perfusion of liver and other organs for the study of microsomal electron-transport and cytochrome P-450 systems. *Methods Enzymol* 1978;52:48-59.
- 36 Meijer AJ, Gimpel JA, Deleeuw GA, Tager JM, Williamson JR: Role of anion translocation across the mitochondrial membrane in the regulation of urea synthesis from ammonia by isolated rat hepatocytes. *J Biol Chem* 1975;250:7728-7738.
- 37 Reinehr R, Becker S, Braun J, Eberle A, Grether-Beck S, Häussinger D: Endosomal acidification and activation of NADPH oxidase isoforms are upstream events in hyperosmolarity-induced hepatocyte apoptosis. *J Biol Chem* 2006;281:23150-23166.
- 38 Hylemon PB, Zhou H, Pandak WM, Ren S, Gil G, Dent P: Bile acids as regulatory molecules. *J Lipid Res* 2009;50:1509-1520.
- 39 Häussinger D, Schmitt M, Weiergraber O, Kubitz R: Short-term regulation of canalicular transport. *Semin Liver Dis* 2000;20:307-321.
- 40 Gottesman MM, Pastan I: Biochemistry of multidrug resistance mediated by the multidrug transporter. *Annu Rev Biochem* 1993;62:385-427.
- 41 Mukhopadhyay S, Ananthanarayanan M, Stieger B, Meier PJ, Suchy FJ, Anwer MS: Sodium taurocholate cotransporting polypeptide is a serine, threonine phosphoprotein and is dephosphorylated by cyclic adenosine monophosphate. *Hepatology* 1998;28:1629-1636.
- 42 Dranoff JA, McClure M, Burgstahler AD, Denson LA, Crawford AR, Crawford JM, Karpen SJ, Nathanson MH: Short-term regulation of bile acid uptake by microfilament-dependent translocation of rat ntcp to the plasma membrane. *Hepatology* 1999;30:223-229.
- 43 Kubitz R, Warskulat U, Schmitt M, Häussinger D: Dexamethasone- and osmolarity-dependent expression of the multidrug-resistance protein 2 in cultured rat hepatocytes. *Biochem J* 1999;340:585-591.
- 44 Dawson PA, Lan T, Rao A: Bile acid transporters. *J Lipid Res* 2009;50:2340-2357.
- 45 Trauner M, Boyer JL: Bile salt transporters: molecular characterization, function, and regulation. *Physiol Rev* 2003;83:633-671.
- 46 Anwer MS, Stieger B: Sodium-dependent bile salt transporters of the SLC10A transporter family: more than solute transporters. *Pflugers Arch* 2014;466:77-89.
- 47 Claro da Silva T, Polli JE, Swaan PW: The solute carrier family 10 (SLC10): beyond bile acid transport. *Mol Aspects Med* 2013;34:252-269.

Mayer et al.: TUDC Protects from GCDC-Induced Ntcp Internalization in the Perfused Rat Liver

- 48 Cuperus FJ, Claudel T, Gautherot J, Halilbasic E, Trauner M: The role of canalicular ABC transporters in cholestasis. *Drug Metab Dispos* 2014;42:546-560.
- 49 Roma MG, Crocenzi FA, Mottino AD: Dynamic localization of hepatocellular transporters in health and disease. *World J Gastroenterol* 2008;14:6786-6801.
- 50 Reinehr R, Becker S, Keitel V, Eberle A, Grether-Beck S, Häussinger D: Bile salt-induced apoptosis involves NADPH oxidase isoform activation. *Gastroenterology* 2005;129:2009-2031.
- 51 Muhlfeld S, Domanova O, Berlage T, Stross C, Helmer A, Keitel V, Häussinger D, Kubitz R: Short-term feedback regulation of bile salt uptake by bile salts in rodent liver. *Hepatology* 2012;56:2387-2397.
- 52 Rodrigues CM, Fan G, Wong PY, Kren BT, Steer CJ: Ursodeoxycholic acid may inhibit deoxycholic acid-induced apoptosis by modulating mitochondrial transmembrane potential and reactive oxygen species production. *Mol Med* 1998;4:165-178.
- 53 Mukhopadhyay S, Ananthanarayanan M, Stieger B, Meier PJ, Suchy FJ, Anwer MS: cAMP increases liver Na⁺-taurocholate cotransport by translocating transporter to plasma membranes. *Am J Physiol* 1997;273:G842-848.
- 54 Roelofsen H, Soroka CJ, Keppler D, Boyer JL: Cyclic AMP stimulates sorting of the canalicular organic anion transporter (Mrp2/cMoat) to the apical domain in hepatocyte couplets. *J Cell Sci* 1998;111:1137-1145.
- 55 Misra S, Varticovski L, Arias IM: Mechanisms by which cAMP increases bile acid secretion in rat liver and canalicular membrane vesicles. *Am J Physiol Gastrointest Liver Physiol* 2003;285:G316-324.
- 56 Park SW, Schonhoff CM, Webster CR, Anwer MS: Protein kinase Cdelta differentially regulates cAMP-dependent translocation of NTCP and MRP2 to the plasma membrane. *Am J Physiol Gastrointest Liver Physiol* 2012;303:G657-665.
- 57 Webster CR, Srinivasulu U, Ananthanarayanan M, Suchy FJ, Anwer MS: Protein kinase B/Akt mediates cAMP- and cell swelling-stimulated Na⁺/taurocholate cotransport and Ntcp translocation. *J Biol Chem* 2002;277:28578-28583.
- 58 McConkey M, Gillin H, Webster CR, Anwer MS: Cross-talk between protein kinases Czeta and B in cyclic AMP-mediated sodium taurocholate co-transporting polypeptide translocation in hepatocytes. *J Biol Chem* 2004;279:20882-20888.
- 59 Sarkar S, Bananis E, Nath S, Anwer MS, Wolkoff AW, Murray JW: PKCzeta is required for microtubule-based motility of vesicles containing the ntcp transporter. *Traffic* 2006;7:1078-1091.
- 60 Anwer MS, Gillin H, Mukhopadhyay S, Balasubramanian N, Suchy FJ, Ananthanarayanan M: Dephosphorylation of Ser-226 facilitates plasma membrane retention of Ntcp. *J Biol Chem* 2005;280:33687-33692.
- 61 Webster CR, Blanch C, Anwer MS: Role of PP2B in cAMP-induced dephosphorylation and translocation of NTCP. *Am J Physiol Gastrointest Liver Physiol* 2002;283:G44-50.
- 62 Layden TJ, Schwarz, Boyer JL: Scanning electron microscopy of the rat liver. Studies of the effect of tauroolithocholate and other models of cholestasis. *Gastroenterology* 1975;69:724-738.
- 63 Miyai K, Richardson AL, Mayr W, Javitt NB: Subcellular pathology of rat liver in cholestasis and choleresis induced by bile salts. 1. Effects of lithocholic, 3beta-hydroxy-5-cholenoic, cholic, and dehydrocholic acids. *Lab Invest* 1977;36:249-258.
- 64 Jung W, Gebhardt R, Robenek H: Primary cultures of rat hepatocytes as a model system of canalicular development, biliary secretion, and intrahepatic cholestasis. II. Tauroolithocholate-induced alterations of canalicular morphology and of the distribution of filipin-cholesterol complexes. *Eur J Cell Biol* 1982;29:77-82.
- 65 Baiocchi L, Tisone G, Russo MA, Longhi C, Palmieri G, Volpe A, Almerighi C, Telesca C, Carbone M, Toti L, De Leonardis F, Angelico M: TUDCA prevents cholestasis and canalicular damage induced by ischemia-reperfusion injury in the rat, modulating PKCalpha-ezrin pathway. *Transpl Int* 2008;21:792-800.
- 66 Abernathy CO, Zimmerman HJ, Ishak KG, Utili R, Gillespie J: Drug-induced cholestasis in the perfused rat liver and its reversal by tauroursodeoxycholate: an ultrastructural study. *Proc Soc Exp Biol Med* 1992;199:54-58.